

ROBUST UNLEARNABLE EXAMPLES: PROTECTING DATA AGAINST ADVERSARIAL LEARNING

Shaopeng Fu¹, Fengxiang He¹, Yang Liu², Li Shen¹ & Dacheng Tao¹

¹JD Explore Academy, JD.com Inc, China

²Institute for AI Industry Research, Tsinghua University, China

{shaopengfu15, fengxiang.f.he, mathshenli, dacheng.tao}@gmail.com
liuy03@air.tsinghua.edu.cn

ABSTRACT

The tremendous amount of accessible data in cyberspace face the risk of being unauthorized used for training deep learning models. To address this concern, methods are proposed to make data unlearnable for deep learning models by adding a type of error-minimizing noise. However, such conferred unlearnability is found fragile to adversarial training. In this paper, we design new methods to generate robust unlearnable examples that are protected from adversarial training. We first find that the vanilla error-minimizing noise, which suppresses the informative knowledge of data via minimizing the corresponding training loss, could not effectively minimize the adversarial training loss. This explains the vulnerability of error-minimizing noise in adversarial training. Based on the observation, robust error-minimizing noise is then introduced to reduce the adversarial training loss. Experiments show that the unlearnability brought by robust error-minimizing noise can effectively protect data from adversarial training in various scenarios. The code is available at <https://github.com/fshp971/robust-unlearnable-examples>.

1 INTRODUCTION

Recent advances in deep learning largely rely on various large-scale datasets, which are mainly built upon public data collected from various online resources such as Flickr, Google Street View, and search engines (Lin et al., 2014; Torralba et al., 2008; Netzer et al., 2011). However, the process of data collection might be unauthorized, leading to the risk of misusing personal data for training deep learning models (Zhang & Tao, 2020; He & Tao, 2020). For example, a recent work demonstrates that individual information such as name or email could be leaked from a pre-trained GPT-2 model (Carlini et al., 2020). Another investigation reveals that a company has been continuously collecting facial images from the internet for training commercial facial recognition models (Hill, 2020).

To prevent the unauthorized use of the released data, recent studies suggest poisoning data with imperceptible noise such that the performances of models trained on the modified data be significantly downgraded (Fowl et al., 2021b;a; Yuan & Wu, 2021; Huang et al., 2021). This work focuses on that by Huang et al. (2021). Specifically, they introduce *unlearnable examples* that are crafted from clean data via adding a type of imperceptible *error-minimizing noise* and show impressive protection ability. The error-minimizing noise is designed based on the intuition that an example of higher training loss may contain more knowledge to be learned. Thereby, the noise protects data from being learned via minimizing the corresponding loss to suppress the informative knowledge of data.

However, such an unlearnability conferred by error-minimizing noise is found vulnerable to adversarial training (Huang et al., 2021; Tao et al., 2021), a standard approach towards training robust deep learning models (Madry et al., 2018). In adversarial training, a model trained on the unlearnable data can achieve the same performance as that trained on the clean data. Similar problems are also found in other poisoning-based data protection methods (Fowl et al., 2021b; Yuan & Wu, 2021) (see Fig. 1). These findings bring great challenges to poisoning-based data protection, and further raises the following question: *Can we still make data unlearnable by adding imperceptible noise even under the adversarial training?*

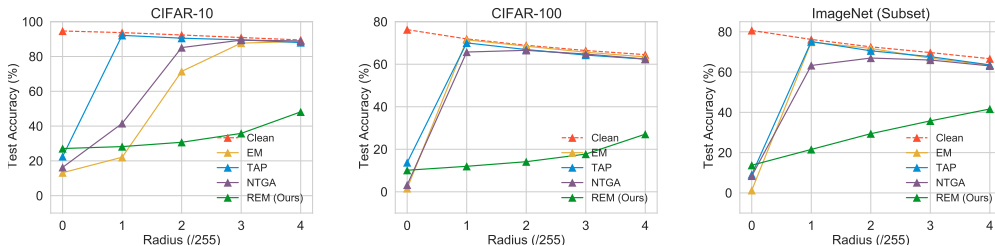


Figure 1: We conduct adversarial training on data protected by different types of noise with varied adversarial perturbation radius ρ_a . EM denotes error-minimizing noise, TAP denotes targeted adversarial poisoning noise, NTGA denotes neural tangent generalization attack noise, and REM denotes robust error-minimizing noise. The curves of test accuracy vs. radius ρ_a are plotted. The results show that as the radius ρ_a increases, (1) the protection brought by EM, NTGA and TAP gradually become invalid, and (2) the proposed REM can still protect data against adversarial learners.

In this paper, we give an affirmative answer that imperceptible noise can indeed stop deep learning models from learning high-level knowledge in an adversarial manner. We first analyze the reason why the unlearnability conferred by error-minimizing noise fails under adversarial training. Adversarial training improves the robustness of models via training them on adversarial examples. However, adversarial examples usually correspond to higher loss, which according to Huang et al. (2021) may contain more knowledge to be learned. Though the error-minimizing noise is designed to minimize the training loss, adversarial examples crafted from unlearnable data could still significantly increase the loss scale (see Fig. 2). Therefore, adversarial training can break the protection brought by error-minimizing noise and still learn knowledge from these data.

Based on the aforementioned analysis, we further deduce that the invalidation of unlearnable examples in adversarial training might be attributed to the error-minimizing noise could not effectively reduce the adversarial training loss. To this end, a new type of noise, named *robust error-minimizing noise*, is designed to protect data against adversarial learners via minimizing the adversarial training loss. Inspired by the strategy of adversarial training and the generation of error-minimizing noise, a min-min-max optimization is designed to train the robust error-minimizing noise generator. Examples crafted by adding robust error-minimizing noise are called *robust unlearnable examples*.

In summary, our work has three main contributions: (1) We present robust error-minimizing noise, which to the best of our knowledge, is the first and currently the only method that can prevent data from being learned in adversarial training. (2) We propose to solve a min-min-max optimization problem to effectively generate robust error-minimizing noise. (3) We empirically verify the effectiveness of robust error-minimizing noise under adversarial training.

2 RELATED WORKS

Adversarial attacks. Adversarial examples are carefully crafted from normal data and can fool machine learning models to behave unexpectedly. It has been found that machine learning models are vulnerable to adversarial examples (Szegedy et al., 2013; Goodfellow et al., 2015; Carlini & Wagner, 2017). Though minor data transformations can mitigate the adversaries of adversarial examples (Lu et al., 2017; Luo et al., 2015), some studies have shown that adversarial examples can further be made resistant to these transformations (Evtimov et al., 2017; Eykholt et al., 2018; Wu et al., 2020b; Athalye et al., 2018; Liu et al., 2019; 2020a). This makes adversarial attacks realistic threats.

To tackle adversarial attacks, adversarial training is proposed to improve the robustness of machine learning models against adversarial examples. Similar to GANs (Goodfellow et al., 2014; Wang et al., 2017; 2019), a standard adversarial training algorithm aims to solve a minimax problem that minimizes the loss function on *most adversarial examples* (Madry et al., 2018). Other advances include TRADE (Zhang et al., 2019), FAT (Zhang et al., 2020), GAIRAT (Zhang et al., 2021), (Song et al., 2020), Jiang et al. (2021), Stutz et al. (2020), Singla & Feizi (2020), Wu et al. (2020a), and Wu et al. (2021). Tang et al. (2021) propose an adversarial robustness benchmark regarding architecture design and training techniques. Some works also attempt to interpret how machine learning models gain robustness (Ilyas et al., 2019; Zhang & Zhu, 2019).

Poisoning attacks. Poisoning attacks aim to manipulate the performance of a machine learning model via injecting malicious poisoned examples into its training set (Biggio et al., 2012; Koh & Liang, 2017; Shafahi et al., 2018; Liu et al., 2020b; Jagielski et al., 2018; Yang et al., 2017; Steinhardt et al., 2017). Though poisoned examples usually appear different from the clear ones (Biggio et al., 2012; Yang et al., 2017), however, recent approaches show that poisoned examples can also be crafted imperceptible to their corresponding origins (Koh & Liang, 2017; Shafahi et al., 2018). A special case of poisoning attacks is the backdoor attack. A model trained on backdoored data may perform well on normal data but wrongly behave on data that contain trigger patterns (Chen et al., 2017; Nguyen & Tran, 2020; 2021; Li et al., 2021; Weng et al., 2020). Compared to other poisoning attacks, backdoor attack is more covert and thus more threatening (Gu et al., 2017).

Recent works suggest employ data poisoning to prevent unauthorized model training. Huang et al. (2021) modify data with error-minimizing noise to stop deep models learning knowledge from the modified data. Yuan & Wu (2021) generate protective noise for data upon an ensemble of neural networks modeled with neural tangent kernels (Jacot et al., 2018), which thus enjoys strong transferability. Fowl et al. (2021a) and Fowl et al. (2021b) employ gradient alignment (Geiping et al., 2020; 2021) and PGD method (Madry et al., 2018) to generate adversarial examples as poisoned data to downgrade the performance of models trained on them. However, Tao et al. (2021) find that existing poisoning-based protection can be easily broken by adversarial training.

3 PRELIMINARIES

Suppose $\mathcal{D} = \{(x_1, y_1), \dots, (x_n, y_n)\}$ is a dataset consists of n samples, where $x_i \in \mathcal{X}$ is the feature of the i -th sample and $y_i \in \mathcal{Y}$ is the corresponding label. A parameterized machine learning model is $f_\theta : \mathcal{X} \rightarrow \mathcal{Y}$, where $\theta \in \Theta$ is the model parameter. Suppose $\ell : \mathcal{Y} \times \mathcal{Y} \rightarrow [0, 1]$ is a loss function. Then, the empirical risk minimization (ERM) aims to approach the optimal model by solving the following optimization problem,

$$\min_{\theta} \frac{1}{n} \sum_{i=1}^n \ell(f_\theta(x_i), y_i). \quad (1)$$

Adversarial training (Madry et al., 2018) improves the robustness of models against adversarial attacks via training them on adversarial examples. A standard adversarial training aims to solve the following min-max problem,

$$\min_{\theta} \frac{1}{n} \sum_{i=1}^n \max_{\|\delta_i\| \leq \rho_a} \ell(f_\theta(x_i + \delta_i), y_i), \quad (2)$$

where $\rho_a > 0$ is the adversarial perturbation radius and $(x_i + \delta_i)$ is the most adversarial example within the ball sphere centered at x_i with radius ρ_a . Usually, a larger radius ρ_a implies stronger adversarial robustness of the trained model.

Unlearnable examples (Huang et al., 2021) is a type of data that deep learning models could not effectively learn informative knowledge from them. Models trained on unlearnable examples could only achieve severely low performance. The generation of unlearnable examples contains two steps. Firstly, train an error-minimizing noise generator f'_θ via solving the following optimization problem,

$$\min_{\theta} \frac{1}{n} \sum_{i=1}^n \min_{\|\delta_i\| \leq \rho_u} \ell(f'_\theta(x_i + \delta_i), y_i), \quad (3)$$

where ρ_u is the defensive perturbation radius that forces the generated error-minimizing noise to be imperceptible. Then, an unlearnable example (x', y) is crafted via adding error-minimizing noise generated by the trained noise generator f'_θ to its clean counterpart (x, y) , where $x' = x + \arg \min_{\|\delta\| \leq \rho_u} \ell(f'_\theta(x + \delta), y)$. The intuition behind this is, a smaller loss may imply less knowledge that could be learned from an example. Thus, error-minimizing noise aims to make data unlearnable via reducing the corresponding training loss. It is worth noting that once the unlearnable data is released publicly, the data defender could not modify the data any further.

Projected gradient descent (PGD) (Madry et al., 2018) is a standard approach for solving the inner maximization and minimization problems in Eqs. (2) and (3). It performs iterative projection

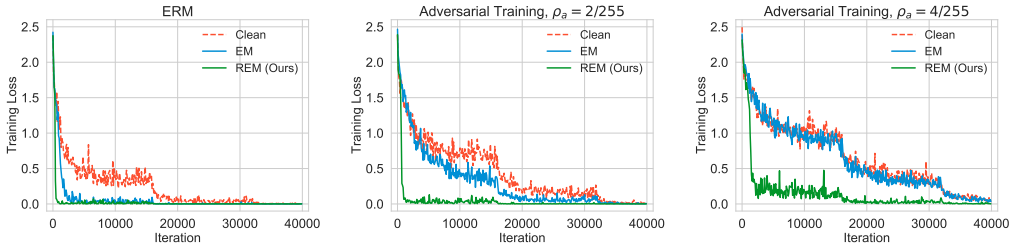


Figure 2: The training loss curves of ERM training and adversarial training on CIFAR-10. Lower training losses suggest stronger unlearnability of data. The results show that: (1) error-minimizing noise could not reduce the training loss as effectively as that in ERM training; (2) robust error-minimizing noise can preserve the training loss in significantly low levels across various learning scenarios. These observations suggest that robust error-minimizing noise is more favorable in preventing data from being learned via adversarial training.

updates to search for the optimal perturbation as follows,

$$\delta^{(k)} = \prod_{\|\delta\| \leq \rho} \left[\delta^{(k-1)} + c \cdot \alpha \cdot \text{sign} \left(\frac{\partial}{\partial \delta} l(f_{\theta}(x + \delta^{(k-1)}), y) \right) \right],$$

where k is the current iteration step (K steps at all), $\delta^{(k)}$ is the perturbation found in the k -th iteration, $c \in \{-1, 1\}$ is a factor for controlling the gradient direction, α is the step size, and $\prod_{\|\delta\| \leq \rho}$ means the projection is calculated in the ball sphere $\{\delta : \|\delta\| \leq \rho\}$. The final output perturbation is $\delta^{(K)}$. Throughout this paper, the coefficient c is set as 1 when solving maximization problems and -1 when solving minimization problems.

4 ROBUST UNLEARNABLE EXAMPLES

In this section, we first illustrate the difficulty of reducing adversarial training loss with error-minimizing noise, and then introduce robust unlearnable examples to tackle the raised challenge.

4.1 ERROR-MINIMIZING NOISE IN ADVERSARIAL TRAINING

Error-minimizing noise prevents unauthorized model training via reducing the corresponding loss to suppress the learnable knowledge of data. However, the goal of reducing training loss may be at odds with that of adversarial training. Recall Eq. (2), adversarial examples usually correspond to higher training losses than that of the clean data, which according to Huang et al. (2021) may contain more knowledge to be learned. Even if error-minimizing noise presents, crafting adversarial examples from unlearnable data could still significantly increase the training loss.

To better illustrate this phenomenon, we conduct adversarial training on clean data and unlearnable data with different adversarial perturbation radius ρ_a . The training losses along the training process are collected and plotted in Fig. 2. From the figure, it can be found that error-minimizing noise could not reduce the training loss as effectively as that in ERM training. Furthermore, as the adversarial perturbation radius ρ_a increases, the adversarial training loss curves on unlearnable data eventually coincide with that on clean data. These observations suggest that adversarial training can effectively recover the knowledge of data protected by error-minimizing noise, which makes the conferred unlearnability invalid.

4.2 ROBUST ERROR-MINIMIZING NOISE

Motivated by the empirical study in Section 4.1, we propose a type of imperceptible noise, named robust error-minimizing noise, to protect data against adversarial learners. Robust error-minimizing noise is designed to minimize the adversarial training loss during adversarial training, which intuitively can barrier the knowledge learning process in adversarial training. Examples crafted via adding robust error-minimizing noise are named robust unlearnable examples.

Similar to that in Huang et al. (2021), the generation of robust error-minimizing noise also needs to first train a noise generator f'_θ . Inspired by the adversarial training loss in Eq. (2) and the objective function for training error-minimizing noise generator in Eq. (3), a min-min-max optimization process is designed to train the robust error-minimizing noise generator f'_θ as follows,

$$\min_{\theta} \frac{1}{n} \sum_{i=1}^n \min_{\|\delta_i^u\| \leq \rho_u} \max_{\|\delta_i^a\| \leq \rho_a} \ell(f'_\theta(x_i + \delta_i^u + \delta_i^a), y_i), \quad (4)$$

where the defensive perturbation radius ρ_u forces the generated noise to be imperceptible, and the adversarial perturbation radius ρ_a controls the protection level of the noise against adversarial training. The idea behind Eq. (4) is, we aim to find a “safer” defensive perturbation δ_i^{u*} such that the adversarial example crafted from the protected sample point $(x_i + \delta_i^{u*})$ would not increase the training loss too much. As a result, the adversarial learner could not extract much knowledge from the data protected by this safer defensive perturbation.

For the choices of the two perturbation radii ρ_u and ρ_a , we notice that when $\rho_u \leq \rho_a$, the following inequality holds for each summation term in Eq. (4),

$$\min_{\|\delta_i^u\| \leq \rho_u} \max_{\|\delta_i^a\| \leq \rho_a} \ell(f'_\theta(x_i + \delta_i^u + \delta_i^a), y_i) \geq \ell(f'_\theta(x_i), y_i).$$

The above inequality suggests that when $\rho_u \leq \rho_a$, the generated defensive noise δ_i^u could not suppress any learnable knowledge of data even in ERM training. Thereby, to help the generated noise gain remarkable protection ability, the radius ρ_u should be set larger than ρ_a .

4.3 ENHANCING THE STABILITY OF THE NOISE

However, the unlearnability conferred by the noise generated via Eq. (4) is found to be fragile to minor data transformation. For example, standard data augmentation (Shorten & Khoshgoftaar, 2019) can easily make the conferred unlearnability invalid (see Section 5.2). To this end, we adopt the *expectation over transformation* technique (EOT; Athalye et al. 2018) into the generation of robust error-minimizing noise. EOT is a stability-enhancing technique that was first proposed for adversarial examples (Evtimov et al., 2017; Eykholt et al., 2018; Athalye et al., 2018). Since adversarial examples and robust unlearnable examples are similar to some extent, it is likely that EOT can also help to improve the stability of robust error-minimizing noise.

Suppose T is a given distribution over a set of some transformation functions $\{t : \mathcal{X} \rightarrow \mathcal{X}\}$. Then, the objective function for training robust error-minimizing noise generator with EOT is adapted from Eq. (4) as follows,

$$\min_{\theta} \frac{1}{n} \sum_{i=1}^n \min_{\|\delta_i^u\| \leq \rho_u} \mathbb{E}_{t \sim T} \max_{\|\delta_i^a\| \leq \rho_a} \ell(f'_\theta(t(x_i + \delta_i^u) + \delta_i^a), y_i). \quad (5)$$

Eq. (5) suggests that, when searching for the defensive perturbation δ_i^u , one needs to minimize several adversarial losses of a set of the transformed examples rather than only minimize the adversarial losses of single examples. After finishing training the noise generator via Eq. (5), the robust unlearnable example (x', y) for a given data point (x, y) is generated as

$$x' = x + \arg \min_{\|\delta^u\| \leq \rho_u} \mathbb{E}_{t \sim T} \max_{\|\delta^a\| \leq \rho_a} \ell(f'_\theta(t(x + \delta^u) + \delta^a), y).$$

4.4 EFFICIENTLY TRAINING THE NOISE GENERATOR

To train the robust error-minimizing noise generator with Eq. (5), we employ PGD to solve the inner minimization and maximization problems. The main challenge of this approach is the gradient calculation of the inner maximization function.

Specifically, the inner maximization function in Eq. (5) usually does not have an analytical solution. As a result, its gradient calculation could not be directly handled by modern Autograd systems such as PyTorch and TensorFlow. Toward this end, we approximate the gradient via first calculating the optimal perturbation $\delta_i^{a*} = \arg \max_{\|\delta_i^a\| \leq \rho_a} \ell(f'_\theta(t(x_i + \delta_i^u) + \delta_i^a), y_i)$ with PGD, and then approximating the gradient of the maximization function by $\frac{\partial}{\partial \delta_i^a} \ell(f'_\theta(t(x_i + \delta_i^u) + \delta_i^{a*}), y_i)$.

Algorithm 1 Training robust error-minimizing noise generator with Eq. (5)

Input: Training data set \mathcal{D} , training iteration M ,

- 1: PGD parameters ρ_u, α_u and K_u for solving the minimization problem,
- 2: PGD parameters ρ_a, α_a and K_a for solving the maximization problem,
- 3: The data transformation distribution T ,
- 4: the number of sampling time J when approximating the gradient of the expectation function.

Output: Robust error-minimizing noise generator f'_θ .

- 5: Initialize source model parameter θ .
- 6: **for** i **in** $1, \dots, M$ **do**
- 7: Sample a minibatch $(x, y) \sim \mathcal{D}$.
- 8: Initialize δ^u .
- 9: **for** k **in** $1, \dots, K_u$ **do**
- 10: **for** j **in** $1, \dots, J$ **do**
- 11: Sample a transformation function $t_j \sim T$.
- 12: $\delta_j^a \leftarrow \text{PGD}(t_j(x + \delta^u), y, f'_\theta, \rho_a, \alpha_a, K_a)$ \triangleright Finding adversarial perturbation.
- 13: **end for**
- 14: $g_k \leftarrow \frac{1}{J} \sum_{j=1}^J \frac{\partial}{\partial \delta^u} \ell(f'_\theta(t_j(x + \delta^u) + \delta_j^a), y)$
- 15: $\delta^u \leftarrow \prod_{\|\delta\| \leq \rho_u} (\delta^u - \alpha_u \cdot \text{sign}(g_k))$
- 16: **end for**
- 17: Sample a transformation function $t \sim T$.
- 18: $\delta^a \leftarrow \text{PGD}(t(x + \delta^u), y, f'_\theta, \rho_a, \alpha_a, K_a)$
- 19: Update source model parameter θ based on minibatch $(t(x + \delta^u) + \delta^a, y)$.
- 20: **end for**
- 21: **return** f'_θ

Therefore, when searching for the optimal defensive perturbation δ_i^{u*} with PGD, one can follow Athalye et al. (2018) to approximate the gradient of the expectation of transformation via first sampling several transformation functions and then averaging the gradients of the corresponding inner maximization function. The gradients of the inner maximization function are approximated via the aforementioned gradient approximation method. Finally, the overall procedures for solving Eq. (5) are presented as Algorithm 1. The effect of the robust error-minimizing noise generated based on Algorithm 1 is illustrated in Fig. 2, which verifies the ability of error-minimizing noise of suppressing training loss in adversarial training.

5 EXPERIMENTS

In this section, we conduct comprehensive experiments to verify the effectiveness of the robust error-minimizing noise in preventing data being learned by adversarial learners.

5.1 EXPERIMENT SETUP

Datasets. Three benchmark computer vision datasets, CIFAR-10, CIFAR-100 (Krizhevsky et al., 2009), and an ImageNet subset (consists of the first 100 classes) (Russakovsky et al., 2015), are used in our experiments. The data augmentation technique (Shorten & Khoshgoftaar, 2019) is adopted in every experiment. For the detailed settings of the data augmentation, please see Appendix A.2.

Robust error-minimizing noise generation. Following Huang et al. (2021), we employ ResNet-18 (He et al., 2016) as the source model f'_θ for training robust error-minimizing noise generator with Eq. (5). The L_∞ -bounded noises $\|\delta_u\|_\infty \leq \rho_u$ and $\|\delta_a\|_\infty \leq \rho_a$ are adopted in our experiments. The detailed training settings are presented in Appendix A.3.1.

Baseline methods. The proposed robust error-minimizing noise (**REM**) is compared with three state-of-the-art data protection noises, the error-minimizing noise (**EM**) (Huang et al., 2021), the targeted adversarial poisoning noise (**TAP**) (Fowl et al., 2021b), and the neural tangent generalization attack noise (**NTGA**) (Yuan & Wu, 2021). See Appendix A.3.2 for the detailed generation procedures of every type of noise.

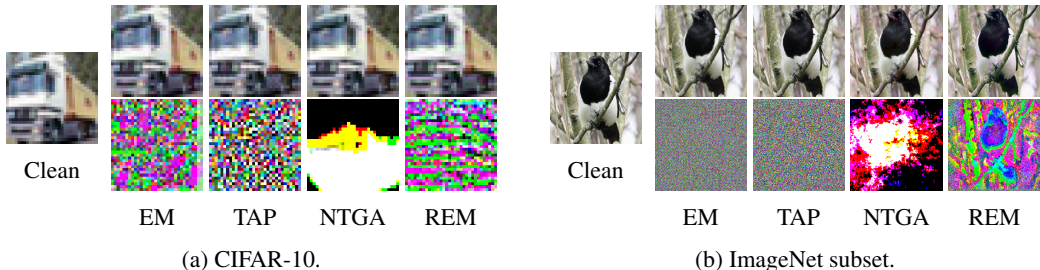


Figure 3: Visualization results of different types of defensive noise as well as the correspondingly crafted examples. EM denotes error-minimizing noise, TAP denotes targeted adversarial poisoning noise, NTGA denotes neural tangent generalization attack noise, and REM denotes robust error-minimizing noise.

Table 1: Test accuracy (%) of models trained on data protected by different defensive noises via adversarial training with different perturbation radii. The defensive perturbation radius ρ_u is set as $8/255$ for every type of noise, while the adversarial perturbation radius ρ_a of REM noise takes various values.

Dataset	Adv. Train. ρ_a	Clean	EM	TAP	NTGA	REM				
						$\rho_a = 0$	1/255	2/255	3/255	4/255
CIFAR-10	0	94.66	13.20	22.51	16.27	15.18	13.05	20.60	20.67	27.09
	1/255	93.74	22.08	92.16	41.53	27.20	14.28	22.60	25.11	28.21
	2/255	92.37	71.43	90.53	85.13	75.42	29.78	25.41	27.29	30.69
	3/255	90.90	87.71	89.55	89.41	88.08	73.08	46.18	30.85	35.80
	4/255	89.51	88.62	88.02	88.96	89.15	86.34	75.14	47.51	48.16
CIFAR-100	0	76.27	1.60	13.75	3.22	1.89	3.72	3.03	8.31	10.14
	1/255	71.90	71.47	70.03	65.74	9.45	4.47	5.68	9.86	11.99
	2/255	68.91	68.49	66.91	66.53	52.46	13.36	7.03	11.32	14.15
	3/255	66.45	65.66	64.30	64.80	66.27	44.93	27.29	17.55	17.74
	4/255	64.50	63.43	62.39	62.44	64.17	61.70	61.88	41.43	27.10
ImageNet Subset	0	80.66	1.26	9.10	8.42	2.54	4.52	6.20	8.88	13.74
	1/255	76.20	74.88	75.14	63.28	12.80	14.68	13.42	14.92	21.58
	2/255	72.52	71.74	70.56	66.96	49.58	33.14	27.06	23.76	29.40
	3/255	69.68	66.90	67.64	65.98	66.68	42.97	41.18	32.16	35.76
	4/255	66.62	63.40	63.56	63.06	64.80	59.32	51.78	41.52	41.66

Model training. We follow Eq. (2) to conduct adversarial training (Madry et al., 2018) on data protected by different defensive noises with different models, including VGG-16 (Simonyan & Zisserman, 2014), ResNet-18, ResNet-50 (He et al., 2016), DenseNet-121 (Huang et al., 2017), and wide ResNet-34-10 (Zagoruyko & Komodakis, 2016). Similar to that in training noise generator, we also focus on L_∞ -bounded noise $\|\rho_a\|_\infty \leq \rho_a$ in adversarial training. Note that when ρ_a takes 0, the adversarial training in Eq. (2) degenerates to the ERM training in Eq. (1). The detailed training settings are given in Appendix A.4.

Metric. We use the test accuracy to assess the data protection ability of the defensive noise. A low test accuracy suggests that the model learned little knowledge from the training data, which thus implies a strong protection ability of the noise.

5.2 EFFECTIVENESS OF ROBUST ERROR-MINIMIZING NOISE

In this section, we study the effectiveness of robust error-minimizing noise from different aspects. We first visualize different defensive noises and the correspondingly crafted examples in Fig. 3. More visualization results can be found in Appendix B.

Different adversarial training perturbation radius. We first add different defensive noises to the entire training set. The defensive perturbation radius ρ_u of every noise is set as $8/255$. Adversarial training is then conducted on both clean data and modified data with ResNet-18 models and different adversarial training perturbation radii ρ_a . Table 1 reports the accuracies of the trained models on clean test data. We have also conducted experiments on noises that generated with a larger defensive perturbation radius $\rho_u = 16/255$, and the results are presented in Table 7 in Appendix C.

Table 2: Test accuracy (%) on CIFAR-10 and CIFAR-100 with different protection percentages. For EM, TAP, and NTGA noises, the perturbation radius ρ_u is set as $8/255$. For REM noise, the perturbation radii ρ_u and ρ_a are set as $8/255$ and $4/255$, respectively.

Dataset	Adv. Train. ρ_a	Noise Type	Data Protection Percentage									
			0%	20%		40%		60%		80%		100%
				Mixed	Clean	Mixed	Clean	Mixed	Clean	Mixed	Clean	
CIFAR-10	2/255	EM		92.26		91.94		91.81		91.14		71.43
		TAP	92.37	92.17	91.30	91.62	90.31	91.32	88.65	91.48	83.37	90.53
		NTGA		92.41		92.19		92.23		91.74		85.13
		REM		92.36		90.22		88.45		82.98		30.69
	4/255	EM		89.60		89.40		89.49		89.10		88.62
		TAP	89.51	89.01	88.17	88.66	86.76	88.40	85.07	88.04	79.41	88.02
		NTGA		89.56		89.35		89.22		89.17		88.96
		REM		89.60		89.34		89.61		88.09		48.16
CIFAR-100	2/255	EM		68.51		68.72		67.96		68.44		68.49
		TAP	68.91	68.05	66.54	67.83	64.21	67.75	58.35	67.27	47.99	66.91
		NTGA		68.52		68.82		68.36		68.71		66.53
		REM		69.00		68.20		60.75		52.33		14.15
	4/255	EM		63.86		64.24		63.62		63.37		63.43
		TAP	64.50	63.21	61.73	63.01	57.61	62.95	53.86	62.90	44.79	62.39
		NTGA		63.48		63.59		63.64		62.83		62.44
		REM		63.75		63.99		64.36		63.05		27.10

As shown in Table 1, when the adversarial training perturbation radius increases, the test accuracy of the model trained on unlearnable data and targeted adversarial poisoned data rapidly increases. On the other hand, the robust error-minimizing noise can always significantly reduce the test accuracy even when adversarial training presents. Furthermore, in the extreme case when the model trained on unlearnable data and targeted adversarial poisoned data achieve the same performance as that trained on clean data, the robust error-minimizing noise can still reduce the test accuracy of the model trained on robust unlearnable data by around 20% to 40%. These results demonstrate the effectiveness of the robust error-minimizing noise against adversarial learners.

Different protection percentages. We then study a more challenging as well as more realistic learning scenario, where only a part of the data are protected by the defensive noise, while the others are clean. Specifically, we randomly select a part of the training data from the whole training set, adding defensive noise to the selected data, and conduct adversarial training with ResNet-18 on the mixed data and the remaining clean data. The defensive perturbation radius for every noise is set as $8/255$, while the adversarial perturbation radius ρ_a of the robust error-minimizing noise is set as $4/255$. The accuracies on clean test data are reported in Table 2. The difference between the test accuracies on mixed data and clean data reflects the knowledge gained from the protected training data. We have also conducted experiments with noises that generated with a larger defensive perturbation radius $\rho_u = 16/255$. The results are reported in Table 8 in Appendix C.

Table 2 shows that when the adversarial training perturbation radius is small, robust error-minimizing noise can effectively protect the selected part of the data. However, when a large adversarial training perturbation radius presents, the protection becomes worthless. This suggests that to protect data against adversarial training with a perturbation radius ρ_a , one has to set the defensive perturbation radius ρ_u of the robust error-minimizing noise to a value that is relatively larger than ρ_a . Table 2 shows that as the data protection percentage decreases, the performance of the trained model increases. This suggests that the model can learn more knowledge from more clean data, which coincides with intuition. Nevertheless, Table 2 further shows that the data protection ability of the robust error-minimizing noise is stronger than that of the error-minimizing noise and the targeted adversarial poisoning noise. This demonstrates that the robust error-minimizing noise is still more favorable than other types of defensive noise when adversarial training presents.

Different model architectures. So far, we have only conduct adversarial training with ResNet-18, which is as same as the source model in the defensive noise generation. We now evaluate the effectiveness of the robust error-minimizing noise under different adversarial learning models. Specifically, we conduct adversarial training with a perturbation radius $4/255$ and five different types of model, including VGG-16, ResNet-18, ResNet-50, DenseNet-121, and wide ResNet-34-10, on data that is protected by noise generated via ResNet-18. Table 3 presents the test accuracies of the

Table 3: Test accuracy (%) of different types of models on CIFAR-10 and CIFAR-100 datasets. The adversarial training perturbation radius is set as $4/255$. The defensive perturbation radius ρ_u of every type of defensive noise is set as $8/255$.

Dataset	Model	Clean	EM	TAP	NTGA	REM	
						$\rho_a = 2/255$	$4/255$
CIFAR-10	VGG-16	87.51	86.48	86.27	86.65	75.97	65.23
	RN-18	89.51	88.62	88.02	88.96	75.14	48.16
	RN-50	89.79	89.28	88.45	88.79	73.59	40.65
	DN-121	83.27	82.44	81.72	80.73	77.82	81.48
	WRN-34-10	91.21	90.05	90.23	89.95	73.98	48.39
CIFAR-100	VGG-16	57.14	56.94	55.24	55.81	56.50	48.85
	RN-18	63.43	64.17	62.39	62.44	61.88	27.10
	RN-50	66.93	66.43	64.44	64.91	61.30	26.03
	DN-121	53.73	53.52	52.93	52.40	54.19	54.48
	WRN-34-10	68.64	68.27	65.80	67.41	64.11	25.04

trained models on CIFAR-10 and CIFAR-100. We have also conducted experiments on noises that generated with a larger defensive perturbation radius $\rho_u = 16/255$. See Table 9 in Appendix C.

Table 3 shows the robust error-minimizing noise generated from ResNet-18 can effectively protect data against various adversarially trained models. However, when the DenseNet-121 model presents, the robust error-minimizing noise could not achieve the same protection performance as that in other scenarios. This may partially be attributed to the limitation of DenseNet-121 itself in adversarial training, as it could not achieve the same generalization ability as those other models on clean data. We will leave further studies on this phenomenon in future works. Nevertheless, the experiment results still demonstrate the effectiveness of robust error-minimizing noise in most cases.

Ablation study on the EOT technique.

In Section 4.3, we propose to employ the EOT technique to enhance the stability of the robust error-minimizing noise in adversarial training. Here, we empirically investigate the effect of EOT. Specifically, we conduct adversarial training with ResNet-18 on datasets protected by robust error noises that are generated with and without the EOT technique, respectively. The accuracies of the trained models on clean test data are reported in Table 4. The results show that without EOT, the generated noise gains no protection ability, which in turn justifies the necessity of employing EOT during the robust error-minimizing noise generation.

Table 4: Ablation study on the EOT technique. Test accuracies (%) of models trained on CIFAR-10 and CIFAR-100 are reported. The defensive perturbation radius ρ_u of the REM noise is set as $8/255$. ‘‘EOT’’ and ‘‘None’’ denote that the noise is generated with and without the EOT technique, respectively.

Dataset	Adv. Train. ρ_a	Clean	REM			
			$\rho_a = 2/255$		$4/255$	
			EOT	None	EOT	None
CIFAR-10	0/255	94.66	20.60	29.15	27.09	18.55
	2/255	92.37	25.41	91.69	30.69	91.76
	4/255	89.51	75.14	89.17	48.16	89.41
CIFAR-100	0/255	76.27	3.03	4.64	10.14	7.03
	2/255	68.91	7.03	68.85	14.15	69.98
	4/255	64.50	61.88	63.51	27.10	63.79

6 CONCLUSION AND FUTURE WORKS

This paper proposes robust error minimizing noise, the first defensive noise that can protect data from being learned by unauthorized adversarial training. We deduce that the error-minimizing noise proposed by Huang et al. (2021) could not prevent unauthorized adversarial training mainly because it can not suppress the training loss in adversarial training based on empirical study. Motivated by this, the robust error-minimizing noise is introduced to effectively reduce the adversarial training loss and thus suppress the learnable knowledge of data in adversarial training. Inspired by the adversarial training loss and the vanilla error-minimizing noise generation, a min-min-max problem is designed for training the robust error-minimizing noise generator, where the expectation over transform technique is adopted to enhance the stability of the generated noise. An important future direction is to establish theoretical foundations for the effectiveness of robust-error minimizing noise. Another interesting direction is to design more efficient robust error-minimizing noise generation methods.

ACKNOWLEDGMENTS

This work is supported by the Major Science and Technology Innovation 2030 “New Generation Artificial Intelligence” key project (No. 2021ZD0111700). Yang Liu is supported in part by the Tsinghua (AIR)-Asiainfo Technologies (China) Research Center under grant No. 20203910074. The authors sincerely appreciate the anonymous ICLR reviewers for their helpful comments.

REFERENCES

- Anish Athalye, Logan Engstrom, Andrew Ilyas, and Kevin Kwok. Synthesizing robust adversarial examples. In *International Conference on Machine Learning*, pp. 284–293. PMLR, 2018.
- Battista Biggio, Blaine Nelson, and Pavel Laskov. Poisoning attacks against support vector machines. In *International Conference on Machine Learning*, pp. 1807–1814, 2012.
- Nicholas Carlini and David Wagner. Towards evaluating the robustness of neural networks. In *2017 IEEE Symposium on Security and Privacy (SP)*, pp. 39–57. IEEE, 2017.
- Nicholas Carlini, Florian Tramer, Eric Wallace, Matthew Jagielski, Ariel Herbert-Voss, Katherine Lee, Adam Roberts, Tom Brown, Dawn Song, Ulfar Erlingsson, et al. Extracting training data from large language models. *arXiv preprint arXiv:2012.07805*, 2020.
- Xinyun Chen, Chang Liu, Bo Li, Kimberly Lu, and Dawn Song. Targeted backdoor attacks on deep learning systems using data poisoning. *arXiv preprint arXiv:1712.05526*, 2017.
- Ivan Evtimov, Kevin Eykholt, Earlene Fernandes, Tadayoshi Kohno, Bo Li, Atul Prakash, Amir Rahmati, and Dawn Song. Robust physical-world attacks on machine learning models. *arXiv preprint arXiv:1707.08945*, 2017.
- Kevin Eykholt, Ivan Evtimov, Earlene Fernandes, Bo Li, Amir Rahmati, Chaowei Xiao, Atul Prakash, Tadayoshi Kohno, and Dawn Song. Robust physical-world attacks on deep learning visual classification. In *Proceedings of the IEEE Conference on Computer Vision and Pattern Recognition*, pp. 1625–1634, 2018.
- Liam Fowl, Ping-yeh Chiang, Micah Goldblum, Jonas Geiping, Arpit Bansal, Wojtek Czaja, and Tom Goldstein. Preventing unauthorized use of proprietary data: Poisoning for secure dataset release. *arXiv preprint arXiv:2103.02683*, 2021a.
- Liam H Fowl, Micah Goldblum, Ping yeh Chiang, Jonas Geiping, Wojciech Czaja, and Tom Goldstein. Adversarial examples make strong poisons. In *Advances in Neural Information Processing Systems*, 2021b.
- Jonas Geiping, Hartmut Bauermeister, Hannah Dröge, and Michael Moeller. Inverting gradients - How easy is it to break privacy in federated learning? In *Advances in Neural Information Processing Systems*, volume 33, pp. 16937–16947, 2020.
- Jonas Geiping, Liam H Fowl, W. Ronny Huang, Wojciech Czaja, Gavin Taylor, Michael Moeller, and Tom Goldstein. Witches’ brew: Industrial scale data poisoning via gradient matching. In *International Conference on Learning Representations*, 2021.
- Ian Goodfellow, Jean Pouget-Abadie, Mehdi Mirza, Bing Xu, David Warde-Farley, Sherjil Ozair, Aaron Courville, and Yoshua Bengio. Generative adversarial nets. In *Advances in Neural Information Processing Systems*, pp. 2672–2680, 2014.
- Ian Goodfellow, Jonathon Shlens, and Christian Szegedy. Explaining and harnessing adversarial examples. In *International Conference on Learning Representations*, 2015.
- Tianyu Gu, Brendan Dolan-Gavitt, and Siddharth Garg. BadNets: Identifying vulnerabilities in the machine learning model supply chain. *arXiv preprint arXiv:1708.06733*, 2017.
- Fengxiang He and Dacheng Tao. Recent advances in deep learning theory. *arXiv preprint arXiv:2012.10931*, 2020.

- Kaiming He, Xiangyu Zhang, Shaoqing Ren, and Jian Sun. Deep residual learning for image recognition. In *Proceedings of the IEEE conference on computer vision and pattern recognition*, pp. 770–778, 2016.
- Kashmir Hill. Meet Clearview AI, the secretive company that might end privacy as we know it. *The New York Times*, 2020.
- Gao Huang, Zhuang Liu, Laurens Van Der Maaten, and Kilian Q Weinberger. Densely connected convolutional networks. In *Proceedings of the IEEE conference on computer vision and pattern recognition*, pp. 4700–4708, 2017.
- Hanxun Huang, Xingjun Ma, Sarah Monazam Erfani, James Bailey, and Yisen Wang. Unlearnable examples: Making personal data unexploitable. In *International Conference on Learning Representations*, 2021.
- Andrew Ilyas, Shibani Santurkar, Dimitris Tsipras, Logan Engstrom, Brandon Tran, and Aleksander Madry. Adversarial examples are not bugs, they are features. In *Advances in Neural Information Processing Systems*, volume 32, 2019.
- Arthur Jacot, Franck Gabriel, and Clément Hongler. Neural tangent kernel: Convergence and generalization in neural networks. *Advances in Neural Information Processing Systems*, 31, 2018.
- Matthew Jagielski, Alina Oprea, Battista Biggio, Chang Liu, Cristina Nita-Rotaru, and Bo Li. Manipulating machine learning: Poisoning attacks and countermeasures for regression learning. In *2018 IEEE Symposium on Security and Privacy (SP)*, pp. 19–35. IEEE, 2018.
- Haoming Jiang, Zhehui Chen, Yuyang Shi, Bo Dai, and Tuo Zhao. Learning to defend by learning to attack. In *Proceedings of The 24th International Conference on Artificial Intelligence and Statistics*, volume 130, pp. 577–585. PMLR, 2021.
- Pang Wei Koh and Percy Liang. Understanding black-box predictions via influence functions. In *International Conference on Machine Learning*, pp. 1885–1894. PMLR, 2017.
- Alex Krizhevsky, Geoffrey Hinton, et al. Learning multiple layers of features from tiny images. 2009.
- Yige Li, Xixiang Lyu, Nodens Koren, Lingjuan Lyu, Bo Li, and Xingjun Ma. Neural attention distillation: Erasing backdoor triggers from deep neural networks. In *International Conference on Learning Representations*, 2021.
- Tsung-Yi Lin, Michael Maire, Serge Belongie, James Hays, Pietro Perona, Deva Ramanan, Piotr Dollár, and C Lawrence Zitnick. Microsoft COCO: Common objects in context. In *European Conference on Computer Vision*, pp. 740–755. Springer, 2014.
- Aishan Liu, Xianglong Liu, Jiabin Fan, Yuqing Ma, Anlan Zhang, Huiyuan Xie, and Dacheng Tao. Perceptual-sensitive GAN for generating adversarial patches. In *Proceedings of the AAAI conference on artificial intelligence*, volume 33, pp. 1028–1035, 2019.
- Aishan Liu, Jiakai Wang, Xianglong Liu, Bowen Cao, Chongzhi Zhang, and Hang Yu. Bias-based universal adversarial patch attack for automatic check-out. In *Proceedings of the European Conference on Computer Vision*, pp. 395–410. Springer, 2020a.
- Sijia Liu, Songtao Lu, Xiangyi Chen, Yao Feng, Kaidi Xu, Abdullah Al-Dujaili, Mingyi Hong, and Una-May O’Reilly. Min-max optimization without gradients: Convergence and applications to black-box evasion and poisoning attacks. In *International Conference on Machine Learning*, pp. 6282–6293. PMLR, 2020b.
- Jiajun Lu, Hussein Sibai, Evan Fabry, and David Forsyth. No need to worry about adversarial examples in object detection in autonomous vehicles. *arXiv preprint arXiv:1707.03501*, 2017.
- Yan Luo, Xavier Boix, Gemma Roig, Tomaso Poggio, and Qi Zhao. Foveation-based mechanisms alleviate adversarial examples. *arXiv preprint arXiv:1511.06292*, 2015.

- Aleksander Madry, Aleksandar Makelov, Ludwig Schmidt, Dimitris Tsipras, and Adrian Vladu. Towards deep learning models resistant to adversarial attacks. In *International Conference on Learning Representations*, 2018.
- Yuval Netzer, Tao Wang, Adam Coates, Alessandro Bissacco, Bo Wu, and Andrew Y Ng. Reading digits in natural images with unsupervised feature learning. 2011.
- Tuan Anh Nguyen and Anh Tran. Input-aware dynamic backdoor attack. In *Advances in Neural Information Processing Systems*, volume 33, pp. 3454–3464, 2020.
- Tuan Anh Nguyen and Anh Tuan Tran. Wanet - Imperceptible warping-based backdoor attack. In *International Conference on Learning Representations*, 2021.
- Olga Russakovsky, Jia Deng, Hao Su, Jonathan Krause, Sanjeev Satheesh, Sean Ma, Zhiheng Huang, Andrej Karpathy, Aditya Khosla, Michael Bernstein, et al. Imagenet large scale visual recognition challenge. *International Journal of Computer Vision*, 115(3):211–252, 2015.
- Ali Shafahi, W. Ronny Huang, Mahyar Najibi, Octavian Suci, Christoph Studer, Tudor Dumitras, and Tom Goldstein. Poison frogs! Targeted clean-label poisoning attacks on neural networks. In *Advances in Neural Information Processing Systems*, volume 31, 2018.
- Connor Shorten and Taghi M Khoshgoftaar. A survey on image data augmentation for deep learning. *Journal of Big Data*, 6(1):1–48, 2019.
- Karen Simonyan and Andrew Zisserman. Very deep convolutional networks for large-scale image recognition. *arXiv preprint arXiv:1409.1556*, 2014.
- Sahil Singla and Soheil Feizi. Second-order provable defenses against adversarial attacks. In *International Conference on Machine Learning*, pp. 8981–8991. PMLR, 2020.
- Chuanbiao Song, Kun He, Jiadong Lin, Liwei Wang, and John E. Hopcroft. Robust local features for improving the generalization of adversarial training. In *International Conference on Learning Representations*, 2020.
- Jacob Steinhardt, Pang Wei Koh, and Percy Liang. Certified defenses for data poisoning attacks. In *Advances in Neural Information Processing Systems*, pp. 3520–3532, 2017.
- David Stutz, Matthias Hein, and Bernt Schiele. Confidence-calibrated adversarial training: Generalizing to unseen attacks. In *International Conference on Machine Learning*, pp. 9155–9166. PMLR, 2020.
- Christian Szegedy, Wojciech Zaremba, Ilya Sutskever, Joan Bruna, Dumitru Erhan, Ian Goodfellow, and Rob Fergus. Intriguing properties of neural networks. *arXiv preprint arXiv:1312.6199*, 2013.
- Shiyu Tang, Ruihao Gong, Yan Wang, Aishan Liu, Jiakai Wang, Xinyun Chen, Fengwei Yu, Xianglong Liu, Dawn Song, Alan Yuille, Philip H.S. Torr, and Dacheng Tao. RobustART: Benchmarking robustness on architecture design and training techniques. *arXiv preprint arXiv:2109.05211*, 2021.
- Lue Tao, Lei Feng, Jinfeng Yi, Sheng-Jun Huang, and Songcan Chen. Better safe than sorry: Preventing delusive adversaries with adversarial training. In *Advances in Neural Information Processing Systems*, 2021.
- Antonio Torralba, Rob Fergus, and William T Freeman. 80 million tiny images: A large data set for nonparametric object and scene recognition. *IEEE Transactions on Pattern Analysis and Machine Intelligence*, 30(11):1958–1970, 2008.
- Chaoyue Wang, Chaohui Wang, Chang Xu, and Dacheng Tao. Tag disentangled generative adversarial network for object image re-rendering. In *Proceedings of the 26th International Joint Conference on Artificial Intelligence (IJCAI)*, pp. 2901–2907, 2017.
- Chaoyue Wang, Chang Xu, Xin Yao, and Dacheng Tao. Evolutionary generative adversarial networks. *IEEE Transactions on Evolutionary Computation*, 23(6):921–934, 2019. doi: 10.1109/TEVC.2019.2895748.

- Cheng-Hsin Weng, Yan-Ting Lee, and Shan-Hung (Brandon) Wu. On the trade-off between adversarial and backdoor robustness. In *Advances in Neural Information Processing Systems*, volume 33, pp. 11973–11983, 2020.
- Boxi Wu, Heng Pan, Li Shen, Jindong Gu, Shuai Zhao, Zhifeng Li, Deng Cai, Xiaofei He, and Wei Liu. Attacking adversarial attacks as a defense. *arXiv preprint arXiv:2106.04938*, 2021.
- Kaiwen Wu, Allen Wang, and Yaoliang Yu. Stronger and faster Wasserstein adversarial attacks. In *International Conference on Machine Learning*, pp. 10377–10387. PMLR, 2020a.
- Tong Wu, Liang Tong, and Yevgeniy Vorobeychik. Defending against physically realizable attacks on image classification. In *International Conference on Learning Representations*, 2020b.
- Chaofei Yang, Qing Wu, Hai Li, and Yiran Chen. Generative poisoning attack method against neural networks. *arXiv preprint arXiv:1703.01340*, 2017.
- Chia-Hung Yuan and Shan-Hung Wu. Neural tangent generalization attacks. In *International Conference on Machine Learning*, pp. 12230–12240. PMLR, 2021.
- Sergey Zagoruyko and Nikos Komodakis. Wide residual networks. *arXiv preprint arXiv:1605.07146*, 2016.
- Hongyang Zhang, Yaodong Yu, Jiantao Jiao, Eric Xing, Laurent El Ghaoui, and Michael Jordan. Theoretically principled trade-off between robustness and accuracy. In *International Conference on Machine Learning*, pp. 7472–7482. PMLR, 2019.
- Jing Zhang and Dacheng Tao. Empowering things with intelligence: A survey of the progress, challenges, and opportunities in artificial intelligence of things. *IEEE Internet of Things Journal*, 8(10):7789–7817, 2020.
- Jingfeng Zhang, Xilie Xu, Bo Han, Gang Niu, Lizhen Cui, Masashi Sugiyama, and Mohan Kankanhalli. Attacks which do not kill training make adversarial learning stronger. In *International Conference on Machine Learning*, pp. 11278–11287. PMLR, 2020.
- Jingfeng Zhang, Jianing Zhu, Gang Niu, Bo Han, Masashi Sugiyama, and Mohan Kankanhalli. Geometry-aware instance-reweighted adversarial training. In *International Conference on Learning Representations*, 2021.
- Tianyuan Zhang and Zhanxing Zhu. Interpreting adversarially trained convolutional neural networks. In *International Conference on Machine Learning*, pp. 7502–7511. PMLR, 2019.

A EXPERIMENT DETAILS

This section provides the experiment details omitted from Section 5.

A.1 HARDWARE DETAILS

The experiments on CIFAR-10 and CIFAR-100 are conducted on 1 GPU (NVIDIA[®] Tesla[®] V100 16GB) and 10 CPU cores (Intel[®] Xeon[®] Processor E5-2650 v4 @ 2.20GHz).

The experiments on ImageNet are conducted on 4 GPU (NVIDIA[®] Tesla[®] V100 16GB) and 40 CPU cores (Intel[®] Xeon[®] Processor E5-2650 v4 @ 2.20GHz).

A.2 DATA AUGMENTATION

We use different data augmentations for different datasets. For CIFAR-10 and CIFAR-100, we perform data augmentation via random flipping, padding 4 pixels on each side, random cropping to 32×32 size, and rescaling per pixel to $[-0.5, 0.5]$ for each image. For the ImageNet subset, we perform data augmentation via random cropping, resizing to 224×224 size, random flipping, and rescaling per pixel to $[-0.5, 0.5]$ for each image.

A.3 DEFENSIVE NOISE GENERATION

Our experiments involve three types of defensive noise, the proposed robust error-minimizing noise, and two baseline methods, error-minimizing noise and adversarial poisoning noise.

Table 5: The settings of PGD (see Eq. (3)) for the noise generations of error-minimizing noise (EM), targeted adversarial poisoning noise (TAP), neural tangent generalization attack noise (NTGA), and robust error-minimizing noise (REM) in different experiments. ρ_u denotes the defensive perturbation radius of different types of noise, while ρ_a denotes the adversarial perturbation radius of the robust error-minimizing noise.

Datasets	Noise Type	α_u	K_u	α_a	K_a
CIFAR-10 CIFAR-100	EM	$\rho_u/5$	10	-	-
	TAP	$\rho_u/125$	250	-	-
	NTGA	$\rho_u/10 \times 1.1$	10	-	-
	REM	$\rho_u/5$	10	$\rho_a/5$	10
ImageNet Subset	EM	$\rho_u/5$	7	-	-
	TAP	$\rho_u/50$	100	-	-
	NTGA	$\rho_u/8 \times 1.1$	8	-	-
	REM	$\rho_u/4$	7	$\rho_a/5$	10

A.3.1 ROBUST ERROR-MINIMIZING NOISE

Following Huang et al. (2021), we employ ResNet-18 (He et al., 2016) as the source model f' for the robust error-minimizing noise generation. The L_∞ -bounded noises $\|\delta_u\|_\infty \leq \rho_u$ and $\|\delta_a\|_\infty \leq \rho_a$ are adopted in our experiments, in which the defensive perturbation radius ρ_u and adversarial perturbation radius ρ_a can take various values. The settings of PGD for solving the inner minimization and maximization problems in Eq. (5) are presented in Table 5.

For CIFAR-10 and CIFAR-100, each source model is trained with SGD for 5,000 iterations, with a batch size of 128, a momentum factor of 0.9, a weight decay factor of 0.0005, an initial learning rate of 0.1, and a learning rate scheduler that decay the learning rate by a factor of 0.1 every 2,000 iterations. For EOT, the data transformation T is set as the data augmentation of the corresponding dataset, and the repeatedly sampling number for expectation estimation is set as 5.

Besides, for the ImageNet subset, each source model is trained with SGD via Eq. (5) for 3,000 iterations, with a batch size of 128, a momentum factor of 0.9, a weight decay factor of 0.0005, an initial learning rate of 0.1, and a learning rate scheduler that decay the learning rate by a factor of 0.1 every 1,200 iterations. For EOT, the data transformation T is set as the data augmentation of the corresponding dataset, and the repeatedly sampling number for expectation estimation is set as 4.

A.3.2 BASELINE METHODS IMPLEMENTATIONS

Two baseline methods are adopted in our experiments as comparisons, including the error-minimizing noise method and the targeted adversarial poisoning noise method. Every method is reproduced on our own.

Error-minimizing noise (Huang et al., 2021). We follow Eq. (3) to train the error-minimizing noise generator. The error-minimizing noise is then generated with the trained noise generator. ResNet-18 model is used as the source model f' . PGD is employed for solving the inner minimization problem in Eq. (3), where the settings of PGD is presented in Table 5. Other hyperparameters for training the noise generator are set the same as that for the robust error-minimizing noise generator in the previous section.

Targeted adversarial poisoning noise (Fowl et al., 2021b). This type of noise is generated via conducting targeted adversarial attack to the model that is trained on clean data, in which the generated adversarial perturbation is used as the adversarial poisoning noise. Specifically, given a fixed model f_0 and a sample (x, y) , the targeted adversarial attack will generate noise via solving the problem $\arg \max_{\|\delta_u\| \leq \rho_u} \ell(f_0(x + \delta_u), g(y))$, where g is a permutation function on the label space \mathcal{Y} . PGD with *differentiable data augmentation* (Geiping et al., 2021) is employed for solving the above problem. The hyper-parameters for the PGD is given in Table 5.

Neural tangent generalization attack noise (Yuan & Wu, 2021). This type of protective noise aims to weaken the generalization ability of the model trained on the modified data. To do this, an ensemble of neural networks is modeled based on neural tangent kernel (NTK) (Jacot et al., 2018), and the NTGA noise is generated upon the ensemble model. As a result, the NTGA noise enjoys remarkable transferability. We use the official code of NTGA¹ to generate this type of noise. Specifically, we employ the FNN model in Yuan & Wu (2021) as the ensemble model. For CIFAR-10 and CIFAR-100, the block size for approximating NTK is set as 4,000. For the ImageNet subset, the block size is set as 100. The hyper-parameters for the PGD are given in Table 5. Other experiment settings follow Yuan & Wu (2021), please refer accordingly.

A.3.3 TIME COSTS OF NOISE GENERATIONS

We calculate the time costs for training different types of noise generators on different datasets. The results are reported in the following Table 6.

Table 6: Time costs for training different defensive noise generators on different datasets.

Dataset	EM	TAP	NTGA	REM
CIFAR-10	0.4h	0.5h	5.2h	22.6h
CIFAR-100	0.4h	0.5h	5.2h	22.6h
ImageNet Subset	3.9h	5.2h	14.6h	51.2h

A.4 MODEL TRAINING DETAILS

We follow Eq. (2) to perform adversarial training (Madry et al., 2018). Similar to that in training noise generator, we also focus on L_∞ -bounded noise $\|\rho_a\|_\infty \leq \rho_a$ in adversarial training.

In every experiment, the model is trained with SGD for 40,000 iterations, with a batch size of 128, a momentum factor of 0.9, a weight decay factor of 0.0005, an initial learning rate of 0.1, and a learning rate scheduler that decays the learning rate by a factor of 0.1 every 16,000 iterations. For CIFAR-10 and CIFAR-100, the steps number K_a and the step size α_a in PGD are set as 10 and $\rho_a/5$. For the ImageNet subset, the steps number K_a and the step size α_a are set as 8 and $\rho_a/4$.

¹The official code of NTGA is available at <https://github.com/lionelmessi6410/ntga>.

B NOISE VISUALIZATION

This section presents more visualization results of different defensive noises.

B.1 CIFAR-10

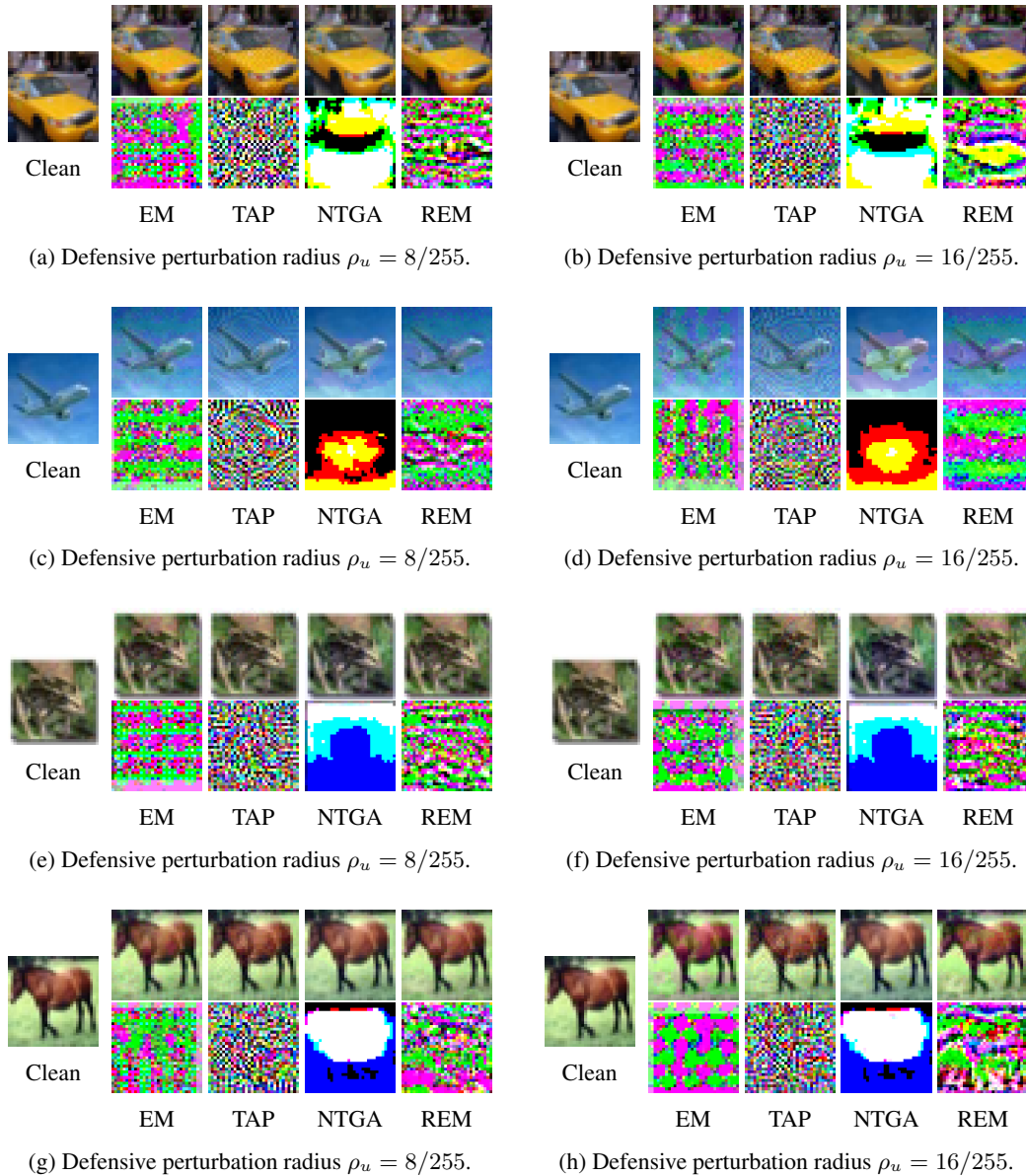


Figure 4: Visualization results of CIFAR-10. Examples of data protected by error-minimizing noise (EM), targeted adversarial poisoning noise (TAP), neural tangent generalization attack noise (NTGA), and robust error-minimizing noise (REM). When ρ_u is set as $8/255$ or $16/255$, the adversarial perturbation radius ρ_a of REM is set as $4/255$ or $8/255$.

B.2 CIFAR-100

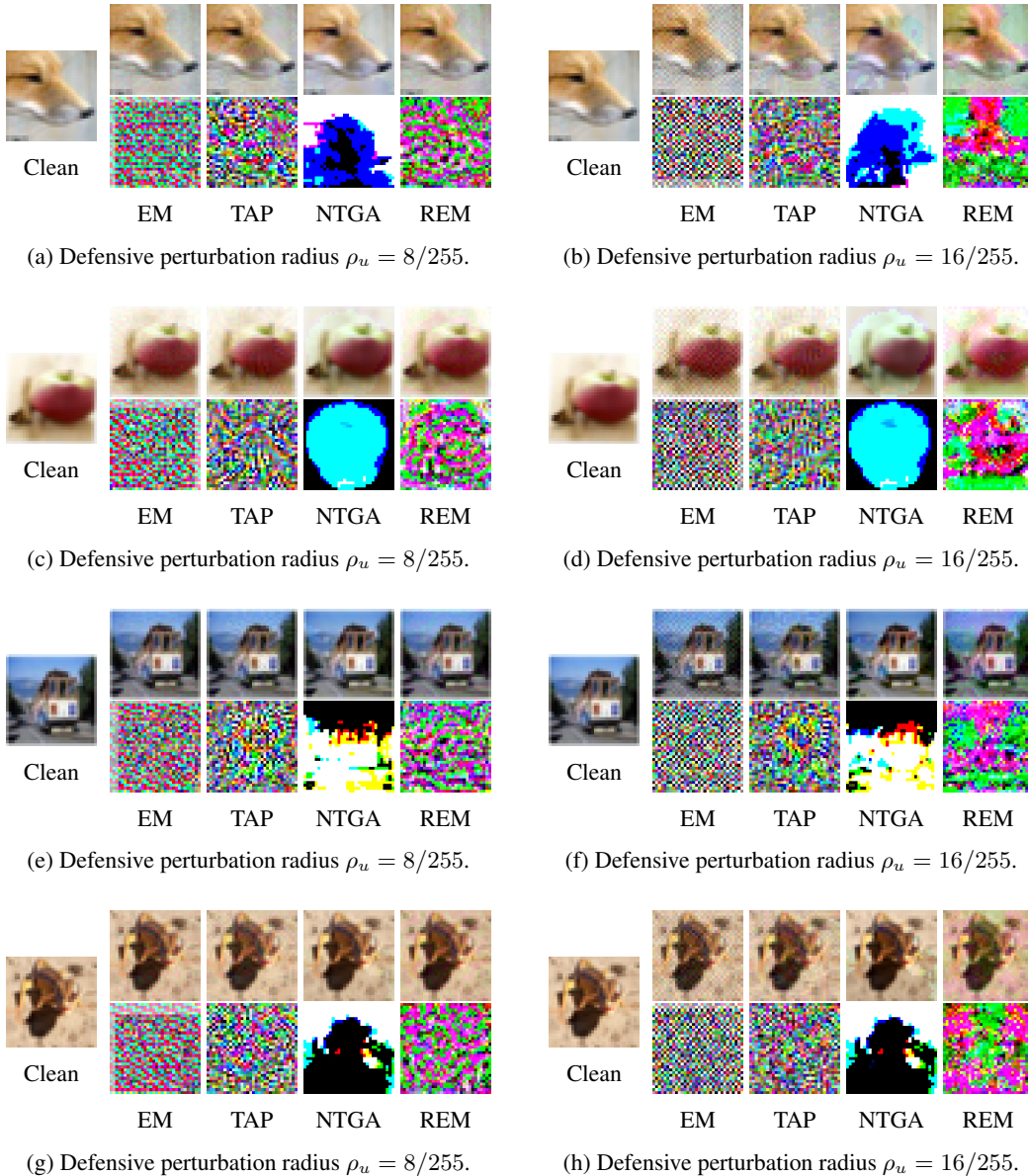


Figure 5: Visualization results of CIFAR-100. Examples of data protected by error-minimizing noise (EM), targeted adversarial poisoning noise (TAP), neural tangent generalization attack noise (NTGA), and robust error-minimizing noise (REM). When ρ_u is set as $8/255$ or $16/255$, the adversarial perturbation radius ρ_a of REM is set as $4/255$ or $8/255$.

B.3 IMAGENET SUBSET

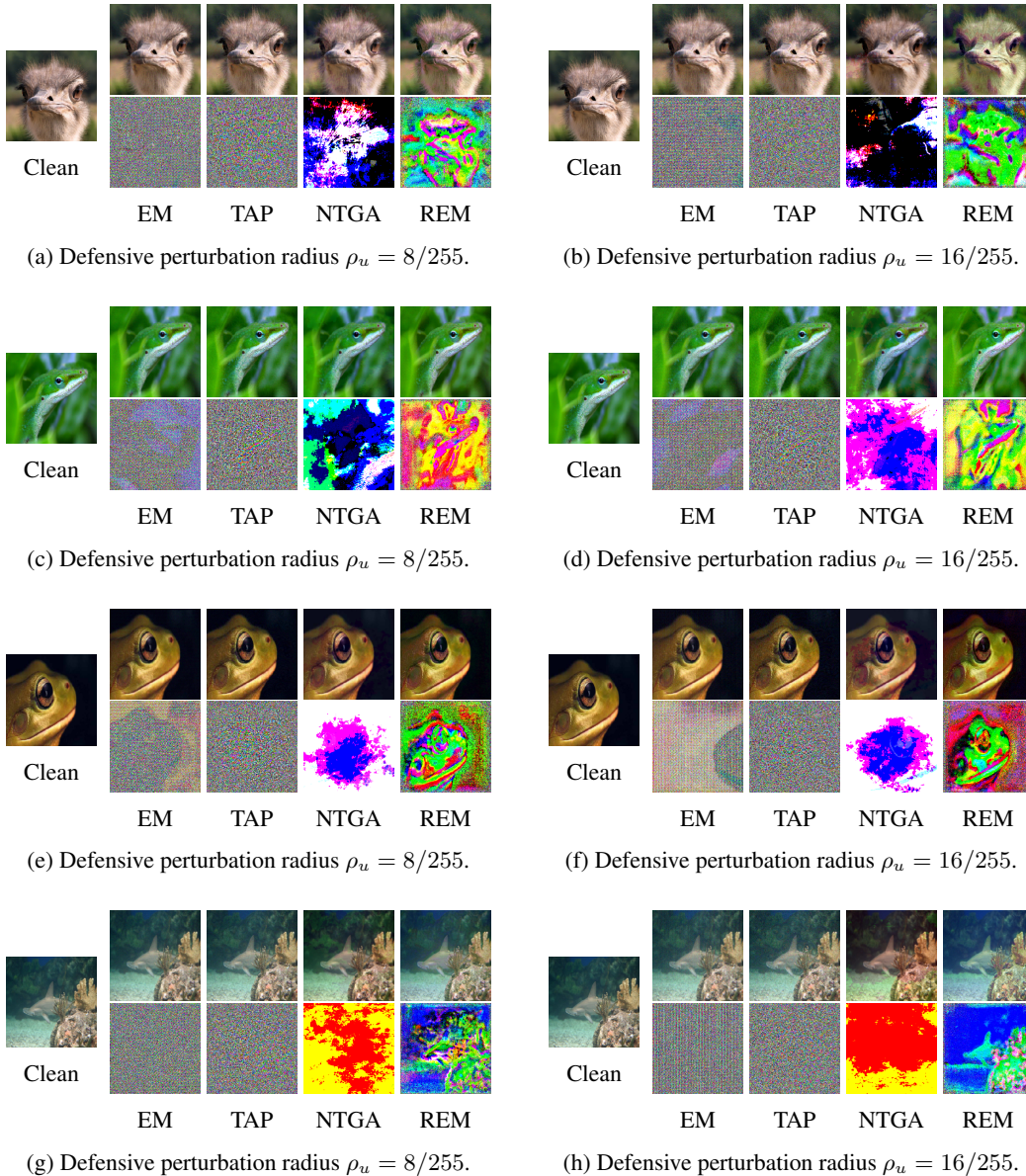


Figure 6: Visualization results of ImageNet subset. Examples of data protected by error-minimizing noise (EM), targeted adversarial poisoning noise (TAP), neural tangent generalization attack noise (NTGA), and robust error-minimizing noise (REM). When ρ_u is set as $8/255$ or $16/255$, the adversarial perturbation radius ρ_a of REM is set as $4/255$ or $8/255$.

C MORE EXPERIMENTS RESULTS

This section collects the additional experiment results for Section 5.2.

Different adversarial training perturbation radius.

Table 7: Test accuracy (%) of models trained on data that are protected by different defensive noises via adversarial training with different perturbation radii. The defensive perturbation radius ρ_u is set as $16/255$ for every type of noise, while the adversarial perturbation radius ρ_a of REM noise takes various values.

Dataset	Adv. Train. ρ_a	Clean	EM	TAP	NTGA	REM				
						$\rho_a = 0$	2/255	4/255	6/255	8/255
CIFAR-10	0	94.66	16.84	11.29	10.91	13.69	13.15	19.51	24.54	24.08
	2/255	92.37	22.46	78.01	19.96	21.17	17.73	20.46	21.89	26.30
	4/255	89.51	41.95	87.60	32.80	45.87	31.18	23.52	26.11	28.31
	6/255	86.90	52.13	85.44	60.64	66.82	58.37	40.25	30.93	31.50
	8/255	84.79	64.71	82.56	74.50	77.08	72.87	63.49	46.92	36.37
CIFAR-100	0	76.27	1.44	4.84	1.54	2.14	4.16	4.27	5.86	11.16
	2/255	68.91	5.21	64.59	5.21	6.68	5.04	4.83	7.86	13.42
	4/255	64.50	35.65	61.48	18.43	28.27	9.80	6.87	9.06	14.46
	6/255	60.86	56.73	57.66	46.30	47.08	35.25	30.16	14.41	17.67
	8/255	58.27	56.66	55.30	50.81	54.23	49.82	54.55	33.86	23.29
ImageNet Subset	0	80.66	1.10	3.96	3.42	2.90	3.40	3.86	5.90	9.72
	2/255	72.52	70.94	70.80	19.90	16.00	8.50	5.66	8.78	14.74
	4/255	66.62	62.16	62.54	41.08	44.12	20.58	11.20	12.46	19.38
	6/255	58.80	55.46	54.68	44.32	55.04	34.04	19.12	16.24	23.14
	8/255	53.12	46.44	46.90	42.78	47.96	44.54	28.20	21.66	26.64

Different data protection percentages.

Table 8: Test accuracy (%) of models trained on CIFAR-10 and CIFAR-100 with different protection percentages. The defensive perturbation radius of every noise is set as $\rho_u = 16/255$. The adversarial perturbation radius of robust error-minimizing noise is set as $8/255$.

Dataset	Adv. Train. ρ_a	Noise Type	Data Protection Percentage										
			0%	20%		40%		60%		80%		100%	
				mixed	clean	mixed	clean	mixed	clean	mixed	clean		
CIFAR-10	4/255	EM		89.45				88.00		86.53			41.95
		TAP		88.80			88.64		87.50		87.83		87.60
		NTGA	89.51	89.63	88.17		88.70	86.76	87.11	85.07	83.32	79.41	32.80
		REM		89.08			87.00		85.05		79.00		28.31
	8/255	EM		84.20			84.37		83.70		82.91		64.71
		TAP		84.24			83.58		83.42		83.09		82.56
		NTGA	84.79	84.62	83.25		84.18	81.54	84.48	79.29	83.26	73.21	74.50
		REM		84.85			83.99		83.15		80.05		36.37
CIFAR-100	4/255	EM		64.27			63.26		63.86		61.45		35.65
		TAP		63.00			62.69		62.65		60.99		61.48
		NTGA	64.50	63.47	61.73		63.09	57.61	63.14	53.86	58.72	44.79	18.43
		REM		63.01			59.90		54.52		47.27		14.46
	8/255	EM		57.44			57.70		57.14		57.27		56.66
		TAP		57.75			57.15		56.32		55.73		55.30
		NTGA	58.27	57.49	55.00		56.35	50.72	55.69	46.29	53.92	39.65	50.81
		REM		57.78			58.12		57.69		55.30		23.29

Different model architectures.

Table 9: Test accuracy (%) of different types of models trained on CIFAR-10 and CIFAR-100. The defensive perturbation radius ρ_u of every defensive noise is set as $16/255$. The adversarial training perturbation radius is set as $8/255$.

Dataset	Model	Clean	EM	TAP	NTGA	REM	
						$\rho_a = 4/255$	$8/255$
CIFAR-10	VGG-16	79.92	63.18	77.73	69.99	63.02	41.17
	RN-18	84.79	64.71	82.56	74.50	63.49	36.37
	RN-50	79.92	61.32	82.59	72.39	57.84	31.91
	DN-121	75.75	67.70	74.35	66.56	62.39	58.70
	WRN-34-10	86.36	65.42	84.19	76.42	64.91	37.51
CIFAR-100	VGG-16	45.67	45.56	43.42	38.83	48.44	22.54
	RN-18	58.27	56.66	55.30	50.81	54.55	23.29
	RN-50	60.15	58.34	56.67	51.88	54.68	21.19
	DN-121	48.28	47.12	46.74	41.05	47.36	42.87
	WRN-34-10	60.95	58.50	57.92	54.47	58.22	22.67

The evolution of the train and test accuracies along the adversarial training process. The curves of train and test accuracies on data protected by different defensive noises are drawn in Fig. 7. The figure shows that robust error-minimizing noise can effectively protect data from being learned along the adversarial training process, while other existing approaches could not. This result further justifies the effectiveness of our proposed method.

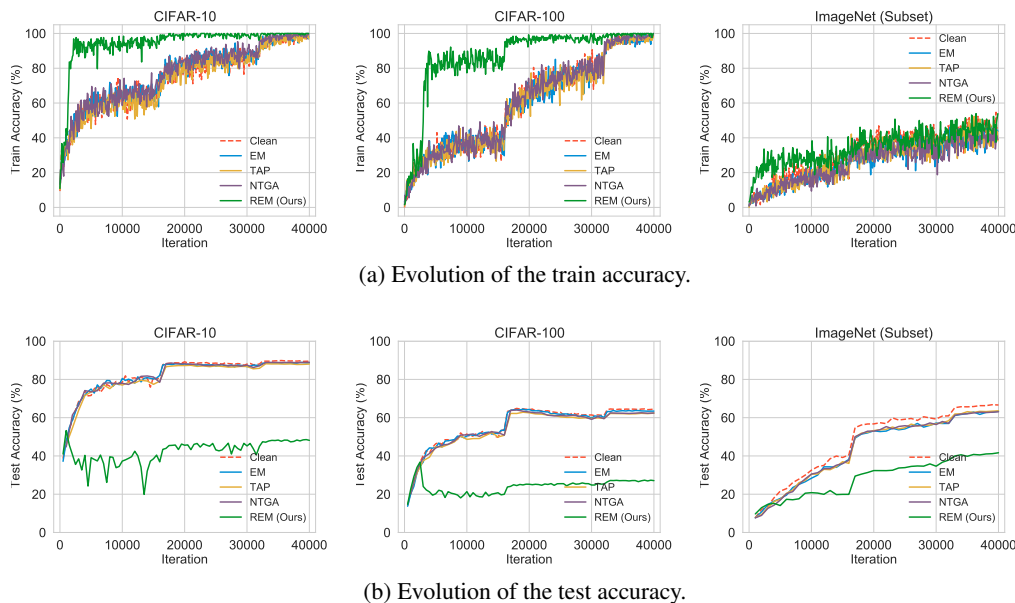


Figure 7: The curves of train and test accuracies to training iteration on data protected by different defensive noises. The defensive perturbation radius ρ_u for every noise is set as $8/255$, while the adversarial perturbation radius ρ_a for REM is set as $4/255$. Besides, the adversarial training perturbation radius is set as $4/255$ in every experiment.

The selections of adversarial perturbation radius ρ_a in robust error-minimizing noise generation. We conduct adversarial training against the robust error-minimizing noises generated with a fixed defensive perturbation radius ρ_u and different adversarial perturbation radii ρ_a . The results are presented Fig. 8, which suggests that setting the adversarial perturbation radius to be half of the defensive perturbation radius would help the noise achieve consistent protection ability against adversarial training with different perturbation radii.

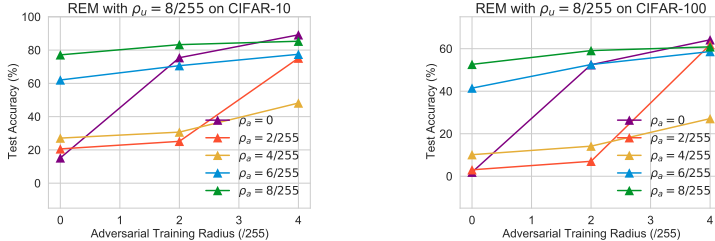


Figure 8: We conduct adversarial training on data protected by different robust error-minimizing noise (REM). The curves of test accuracy vs. adversarial training radius are plotted. The defensive perturbation radius ρ_u for every REM noise is set as $8/255$.

D RESISTANCE TO LOW-PASS FILTERING

This section analyzes the resistance of different protective noises against low-pass filters. We first process each image from the training dataset (can be a clean dataset or protected dataset) with three low-pass filters, mean filter, median filter, and Gaussian filter, respectively. For every filter, the shape of the window is set as 3×3 . We then conduct adversarial training on the processed data with various adversarial training perturbation radii. The experiment results are presented in Table 10.

From the table, we find that when the adversarial training perturbation is small, robust error-minimizing noise can effectively prevent data from being learned. However, when large adversarial training perturbation presents, even robust error-minimizing noise becomes ineffective. Nevertheless, compared with other types of noise, the protection brought by robust error-minimizing noise is stronger in most situations. These results demonstrate that robust error-minimizing is more favorable in protecting data against adversarial learning.

Table 10: Test accuracy (%) of different types of models trained on CIFAR-10 and CIFAR-100 that are processed by different low-pass filters. The defensive perturbation radius ρ_u of every defensive noise is set as $16/255$. The adversarial training perturbation radius is set as $8/255$.

Dataset	Filter	Adv. Train. ρ_a	Clean	EM	TAP	NTGA	REM
CIFAR-10	Mean	2/255	84.25	34.87	82.53	40.26	28.60
		4/255	80.47	56.41	78.87	57.42	40.32
		8/255	74.74	73.42	72.98	67.69	68.70
	Median	2/255	87.04	31.86	85.10	30.87	27.36
		4/255	83.87	49.33	82.31	48.50	34.06
		8/255	78.34	74.02	76.66	67.63	62.14
	Gaussian	2/255	86.78	29.71	85.44	41.85	28.70
		4/255	83.33	52.47	81.83	58.14	35.13
		8/255	77.30	73.84	75.98	70.06	68.19
CIFAR-100	Mean	2/255	52.42	53.07	51.30	26.49	13.89
		4/255	50.89	50.61	50.35	35.46	24.52
		8/255	47.73	46.98	46.62	42.03	44.96
	Median	2/255	57.69	56.35	55.22	18.14	14.08
		4/255	54.77	53.50	53.31	33.05	19.14
		8/255	51.09	49.64	48.86	45.13	40.45
	Gaussian	2/255	56.64	56.49	55.19	29.05	13.74
		4/255	53.44	53.62	53.17	37.39	22.92
		8/255	49.75	49.61	48.59	44.55	47.03

E RESISTANCE TO ADVERSARIAL TRAINING WITH DIFFERENT PERTURBATION NORMS

This section studies the resistance of different protective noises against adversarial training with various perturbation norms. Specifically, when perform adversarial training (*i.e.*, Eq. (2)) on the protected dataset, we set the perturbation norm Eq. (2) as L_1 -norm or L_2 -norm. Other training settings are as same as that presented in Appendix A.4. The experiment results are collected and presented in Table 11, which shows that robust error-minimizing noise can effectively protect data from adversarial training in these situations.

Table 11: Test accuracy (%) of different types of models trained on CIFAR-10 and CIFAR-100. The adversarial training is conducted with different types of perturbation norms. The defensive perturbation radius ρ_u of every defensive noise is set as $16/255$. The adversarial training perturbation radius is set as $8/255$.

Dataset	Norm Type	Adv. Train. ρ_a	Clean	EM	TAP	NTGA	REM
CIFAR-10	L_1 -norm	1000/255	93.61	18.49	53.74	46.78	29.07
		3000/255	90.40	69.82	89.65	84.69	55.98
	L_2 -norm	50/255	92.66	44.11	91.30	73.00	32.90
		100/255	89.91	82.55	88.70	86.75	62.76
CIFAR-100	L_1 -norm	1000/255	72.32	72.03	65.13	47.55	14.49
		3000/255	67.37	66.77	65.64	64.83	40.84
	L_2 -norm	50/255	70.05	69.52	67.45	65.31	17.43
		100/255	65.65	65.25	63.86	63.31	47.16